Crystal Structure of Double Helical Hexitol Nucleic Acids

Ruben Declercq,[†] Arthur Van Aerschot,[‡] Randy J. Read,[§] Piet Herdewijn,[‡] and Luc Van Meervelt*,[†]

Contribution from Biomolecular Architecture, Department of Chemistry, Katholieke Universiteit Leuven, Celestijnenlaan 200F, B-3001 Leuven (Heverlee), Belgium, Laboratory of Medicinal Chemistry, Rega Institute, Katholieke Universiteit Leuven, Minderbroederstraat 10, B-3000 Leuven, Belgium, and Department of Haematology, University of Cambridge, Cambridge Institute for Medical Research, Hills Road, Cambridge CB2 2XY, U.K.

Abstract: A huge variety of chemically modified oligonucleotide derivatives has been synthesized for possible antisense applications. One such derivative, hexitol nucleic acid (HNA), is a DNA analogue containing the standard nucleoside bases, but with a phosphorylated 1′,5′-anhydrohexitol backbone. Hexitol nucleic acids are some of the strongest hybridizing antisense compounds presently known, but HNA duplexes are even more stable. We present here the first high-resolution structure of a double helical nucleic acid with all sugars being hexitols. Although designed to have a restricted conformational flexibility, the hexitol oligomer h(GTGTACAC) is able to crystallize in two different double helical conformations. Both structures display a high x-displacement, normal Watson−Crick base pairing, similar base stacking patterns, and a very deep major groove together with a minor groove with increased hydrophobicity. One of the conformations displays a major groove which is wide enough to accommodate a second HNA double helix resulting in the formation of a double helix of HNA double helices. Both structures show most similarities with the A-type helical structure, the anhydrohexitol chair conformation thereby acting as a good mimic for the furanose C3′-*endo* conformation observed in RNA. As compared to the quasi-linear structure of homo-DNA, the axial position of the base in HNA allows efficient base stacking and hence double helix formation.

Introduction

Many nucleic acid mimics with restricted conformational flexibility are designed and synthesized to target RNA. Striking examples of conformational preorganized furanose nucleic acids with potential antisense activity are locked nucleic acids (LNA)[1] and its stereoisomer α-L-LNA.[2] In LNA, the furanose sugar is preorganized in the C3′-*endo* conformation,[3] and LNA forms an A-type duplex with RNA.[4] α-L-LNA can be considered as a DNA mimic, and the α-L-LNA−RNA duplex conformation is the intermediate between the A and B form.[5] Several other examples exist where the sugar−phosphate backbone is conformationally restricted to obtain preorganized oligomers with a high affinity for RNA, and its principle has been reviewed several times.[6−11]

As compared to DNA, hexitol nucleid acid (HNA) (Figure 1a) can be considered as a backbone modification where an extra methylene group has been inserted between C1′ and O4′ of the β-D-2′-deoxyribose unit. Hexitol nucleic acids form very stable self-complementary duplexes as well as stable duplexes with their natural components.[12] Melting temperature determinations and gel shift experiments show the following order of duplex stability: HNA−HNA > HNA−RNA > HNA−DNA. HNA as a conformationally restricted RNA analogue is an exellent template for nonenzymatic polymerization.[13] It was demonstrated that this polymerization is highly enantioselective[14] which is explained by the rigidity of the HNA template.[15] The hexitol monomers can be incorporated in DNA in an enzymatic way, and they can be used to functionally classify DNA polymerases.[16] On the basis of the monomer conformation

* To whom correspondence should be addressed. Telephone: +32 16 327609. Fax: +32 16 327990. E-mail: Luc.VanMeervelt@ chem.kuleuven.ac.be.
† Department of Chemistry, Katholieke Universiteit Leuven.
‡ Rega Institute, Katholieke Universiteit Leuven.
§ University of Cambridge.

(1) Singh, S. K.; Nielsen, P.; Koshkin, A. A.; Wengel, J. *Chem. Commun.* **1998**, 455−456.
(2) Rajwanshi, V. K.; Hakansson, A. E.; Sorensen, M. D.; Pitch, S.; Singh, S. K.; Kumar, R.; Nielsen, P.; Wengel, J. *Angew. Chem., Int. Ed.* **2000**, *39*, 1656−1659.
(3) Obika, S.; Nanbu, D.; Hari, Y.; Morio, K.; In, Y.; Ishida, T.; Imanishi, T. *Tetrahedron Lett.* **1997**, *38*, 8735−8738.
(4) Bondensgaard, K.; Petersen, M.; Singh, S. K.; Rajwanshi, V. K.; Kumar, R.; Wengel, J.; Jacobsen, J. P. *Chem.-Eur. J.* **2000**, *6*, 2687−2695.
(5) Kvaerno, L.; Wengel, J. *Chem. Commun.* **2001**, 1419−1424.
(6) Egli, M. *Angew. Chem., Int. Ed. Engl.* **1996**, *35*, 1894−1909.
(7) Kool, E. T. *Chem. Rev.* **1997**, *97*, 1473−1487.
(8) Wengel, J. *Acc. Chem. Res.* **1999**, *32*, 301−310.
(9) Herdewijn, P. *Liebigs Ann. Chem.* **1996**, 1337−1348.
(10) Manoharan, M. *Biochim. Biophys. Acta* **1999**, *1489*, 117−130.
(11) Herdewijn, P. *Biochim. Biophys. Acta* **1999**, *1489*, 167−179.
(12) Hendrix, C.; Rosemeyer, H.; De Bouvere, B.; Van Aerschot, A.; Seela, F.; Herdewijn, P. *Chem.-Eur. J.* **1997**, *3*, 110−120.
(13) Kozlov, I. A.; Politis, P. K.; Van Aerschot, A.; Busson, R.; Herdewijn, P.; Orgel, L. E. *J. Am. Chem. Soc.* **1999**, *121*, 2653−2656.
(14) Kozlov, I. A.; Politis, P. K.; Pitsch, S.; Herdewijn, P.; Orgel, L. E. *J. Am. Chem. Soc.* **1999**, *121*, 1108−1109.
(15) Lescrinier, E.; Esnouf, R.; Schraml, J.; Busson, R.; Heus, H.; Hilbers, C.; Herdewijn, P. *Chem. Biol.* **2000**, *7*, 719−731.
(16) Vastmans, K.; Pochet, S.; Peys, A.; Kerremans, L.; Van Aerschot, A.; Hendrix, C.; Marliere, P.; Herdewijn, P. *Biochemistry* **2000**, *39*, 12757−12765.
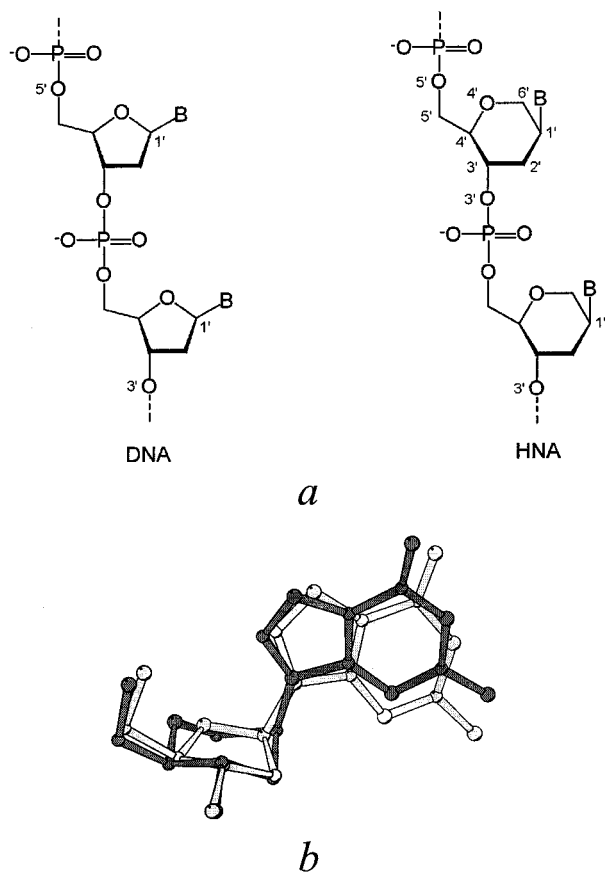
Figure 1. (a) Comparison between the DNA and HNA backbones. (b) A fit of a typical HNA hexitol ring on a sugar ring with C3′-*endo* conformation as found in A-type helical structures.

Table 1. Diffraction Data and Refinement Statistics

	HNA-hex	HNA-trig
Diffraction Data Statistics		
λ (Å)	0.9116	0.8375
resolution (Å)	20.0−2.21	20.0−1.60
space group	$P6_222$	$P3_212$
unique reflections	1344	3345
completeness (%)	83.8 (20.0−2.21)	99.9 (20.0−1.60)
	74.1 (2.25−2.21)	100.0 (1.63−1.60)
multiplicity	16.8	8.5
$R_{merge}(I)$	5.1 (20.0−2.21)	7.1 (20.0−1.60)
	16.8 (2.25−2.21)	17.3 (1.63−1.60)
$I/\sigma(I)$	21.6	13.2
Refinement Statistics		
resolution (Å)	10.0−2.21	20.0−1.60
R value/R_{free} value (%)	23.2/na	17.4/22.9
total number of non-hydrogen atoms	169	169
water molecules	38	40
average B values of HNA (Å²)	44.3	11.1
average B values of water molecules (Å²)	53.2	29.2
Rmsd of bond lengths (Å)	0.018	0.013
Rmsd of bond angles (Å)	0.022	0.019

a na: not available.

analyzed by NMR spectroscopy[17] and X-ray analysis,[18] the incorporation of 1′,5′-anhydrohexitol sugars will greatly influence the three-dimensional structure of HNA duplexes. Circular dichroism measurements together with a molecular dynamics simulation study of an HNA−RNA duplex are indicative of an A form helical structure.[19,20] The HNA duplex structure could provide new insight into how sugar modifications stabilize the duplex structure and hence provide important information for the design of other backbone modifications with novel properties. Here, we present two structures of a short HNA duplex with the self-complementary sequence h(GTGTACAC), showing a different double helical conformation.

Materials and Methods

The HNA octamer was assembled on a LCAA-CPG support functionalized with the 1′,5′-anhydrohexitol analogue (hC). Synthesis was performed at a 10 μmol scale on an ABI-392 synthesizer using the monomethoxytritylated nucleoside phosphoramidite analogues at 0.12 M concentration. The standard protocol was slightly adapted with extension of the coupling time to 10 min and a 5 min detritylation step. Standard deprotection was followed by anion exchange purification at pH 12 on a Mono Q column HR 10/10 (Pharmacia) with a NaCl

gradient in five runs. Gel filtration on a Biogel P2 column (280 × 25 mm, exclusion limit 1800 Da) afforded the purified material as its sodium salt.

Crystals of the HNA octamer h(GTGTACAC) were obtained by hanging drop vapor diffusion using a 24-matrix screen optimized for the crystallization of nucleic acid fragments.[21] Hexagonal-shaped crystals were grown at 277 K. Next 2 μL of a 2.4 mM oligomer solution was mixed with an equal volume containing 10% (v/v) MPD, 12 mM spermine hydrochloride, 80 mM K⁺, 20 mM Ba²⁺, and 40 mM cacodylate buffered at pH 7.0 and equilibrated against 0.5 mL of reservoir solution of 35% (v/v) MPD. These crystals belong to space group $P6_222$ with cell constants $a = 36.36$ Å and $c = 69.12$ Å. A large enough needle-shaped crystal was found after 6 months in similar conditions, be it with a single strand concentration of 2.2 mM, a crystallization temperature of 289 K, and using a thin oil layer (0.1 mL) on top of the reservoir solution to reduce the rate of vapor diffusion [Al's Oil, Hampton Research]. This crystal belongs to space group $P3_212$ with cell constants $a = 33.04$ Å and $c = 38.92$ Å. Crystals were flash-cooled to 100 K, and data were collected at the EMBL beamlines X11 and BW7B at the DORIS storage ring in Hamburg. Data were integrated and reduced with DENZO and SCALEPACK.[22]

In both space groups, the asymmetric unit consists of a single HNA strand. The HNA-hex structure was solved by molecular replacement with Replace[23] using the HNA strand of an HNA−RNA duplex built by molecular dynamics calculations[20] as an initial model. In an extensive series of translation searches using orientations obtained from rotation searches with different choices of parameters, one solution stood out with a significantly higher correlation coefficient and lower R factor. The HNA-trig structure was solved by likelihood-based molecular replacement,[24] using the HNA-hex structure as a model. Because the overall curvature of the double helix differed significantly, clear results were obtained using a half duplex as a model, but not using a single strand. Both solutions were first subjected to a rough energy minimization using X-PLOR.[25] Further refinement on F^2 was done using SHELXL-97.[26] Diffraction data and refinement statistics are presented in Table 1.

(17) Verheggen, I.; Van Aerschot, A.; Toppet, S.; Snoeck, R.; Janssen, G.; Balzarini, J.; De Clercq, E.; Herdewijn, P. *J. Med. Chem.* **1993**, *36*, 2033−2040.
(18) Declercq, R.; Herdewijn, P.; Van Meervelt, L. *Acta Crystallogr.* **1996**, *C52*, 1213−1215.
(19) Hendrix, C.; Rosemeyer, H.; Verheggen, I.; Seela, F.; Van Aerschot, A.; Herdewijn, P. *Chem.-Eur. J.* **1997**, *3*, 1513−1520.
(20) De Winter, H.; Lescrinier, E.; Van Aerschot, A.; Herdewijn, P. *J. Am. Chem. Soc.* **1998**, *120*, 5381−5394.

(21) Berger, I.; ChulHee, K.; Sinha, N.; Wolters, M.; Rich, A. *Acta Crystallogr.* **1996**, *D52*, 465−468.
(22) Otwinowski, Z.; Minor, W. *Methods Enzymol.* **1997**, *276*, 307−326.
(23) Tong, L.; Rossmann, M. G. *Methods Enzymol.* **1997**, *276*, 594−611.
(24) Read, R. J. *Acta Crystallogr.* **2001**, *D57*, 1373−1382.
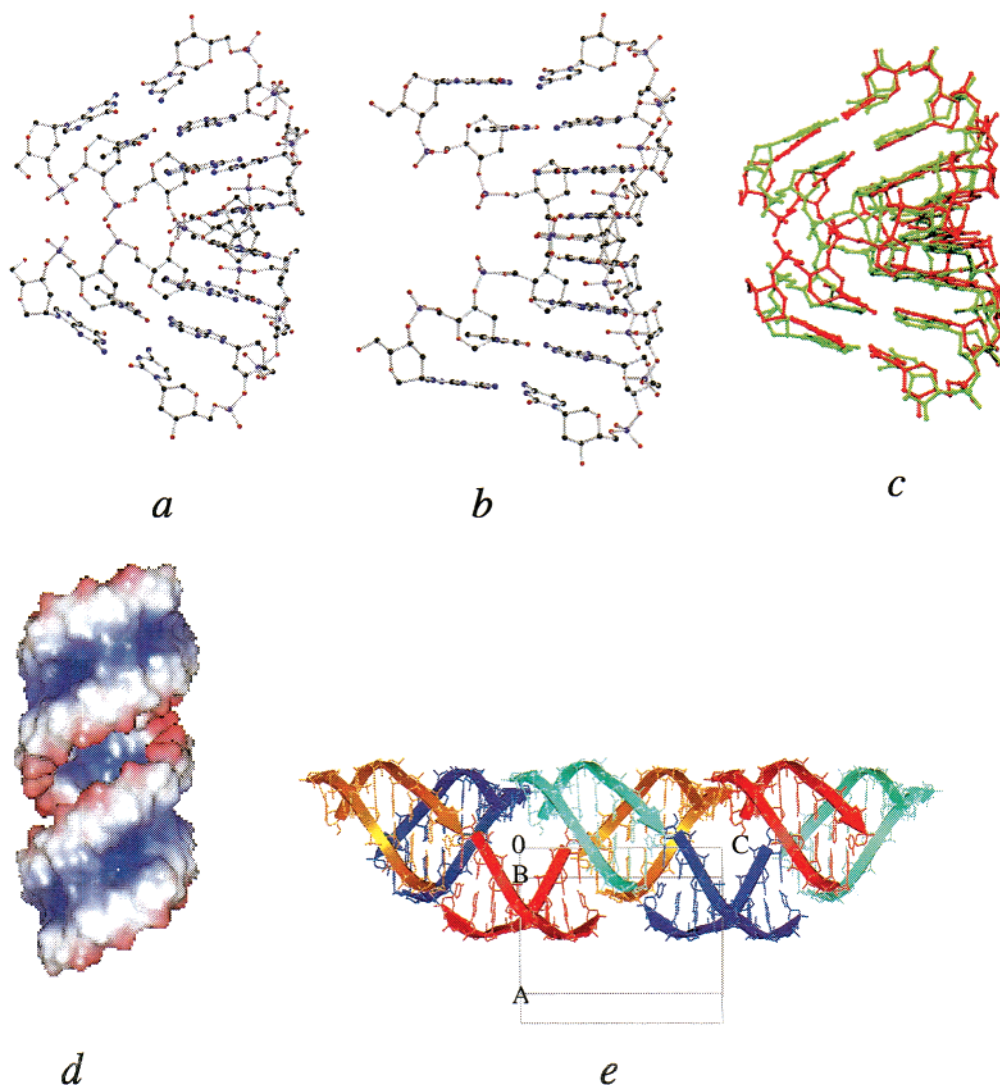
Figure 2. The global helical structure of the HNA octamer h(GTGTACAC) crystallized in the space group $P6_2 22$ (HNA-hex, (a)) and the space group $P3_2 12$ (HNA-trig, (b)). A color coding according to the atom type was applied. (c) Overlay of the P atoms of the HNA-hex duplex (red) to those of a canonical RNA duplex (green) with the same sequence. (d) The solvent accessible surface area of approximately one and a half helical turns of the HNA double helix based on the HNA-hex crystal structure. The surface was calculated using a solvent probe radius of 1.4 Å. The surface color coding is following the electrostatic potential imaged with positive potential in blue and negative potential in red. The diameter of the HNA helix is ∼19 Å. The model was constructed by least-squares fitting of base pair A7•T10 onto G1•C16 of another duplex; overlapping residues were removed, and minor deviations of the standard phosphate geometry were corrected by molecular mechanics minimization.[25] (e) The crystal packing of h(GTGTACAC) in the $P3_2 12$ structure (HNA-trig) giving rise to a "double helix of double helices". The unit cell is outlined in gray.

The atomic coordinates have been deposited in the Protein Data Bank (PDB ID codes 481D, 1D7Z) and in the Nucleic Acid Database (accession codes HD0001, HD0002).

Results and Discussion

Two distinct crystal forms belonging to the space groups $P6_2 22$ (HNA-hex, diffracting to 2.21 Å) and $P3_2 12$ (HNA-trig, diffracting to 1.60 Å) were obtained for the HNA octamer h(GTGTACAC) using vapor-diffusion techniques. Both structures adopt an antiparallel right-handed double helix with all bases engaged in Watson–Crick hydrogen bonding (Figure 2a,b). Although for both structures the hydrogen bonding and C1′···C1′ distances are nearly identical to the standard values

observed in DNA,[27] structural analysis reveals significant differences in their conformation. The average backbone torsion angles display small differences for nearly all torsion angles illustrating the overall difference of backbone conformation. Generally the −*sc*, +*ap*, +*sc*, +*sc*, −*ap*, and −*sc* conformations for α to ζ are observed. An exception is found for the central step in HNA-trig where an extension of the backbone is observed due to a +*ap*, +*ap*, +*ap* conformation for α to γ torsion angles. This correlated transition of α and γ into +*ap* has been observed for several oligonucleotide crystal structures, generally A-type, as well as for solution structures.[28] In most cases, the transition occurs for one isolated step where the central step seems most easily affected. Despite this transition, the base

(25) Brünger, A. T. *X-PLOR: A System for X-ray Crystallography and NMR*, version 3.1; Yale University Press: New Haven, Connecticut, 1992.
(26) Sheldrick, G. M.; Schneider, T. R. *Methods Enzymol.* **1997**, *277*, 319–343.
(27) Saenger, W. In *Principles of Nucleic Acid Structure*; Cantor, C. R., Ed.; Springer-Verlag: New York, 1984; pp 116–126.
(28) Conn, G. L.; Brown, T.; Leonard, G. A. *Nucleic Acids Res.* **1999**, *27*, 555–561.
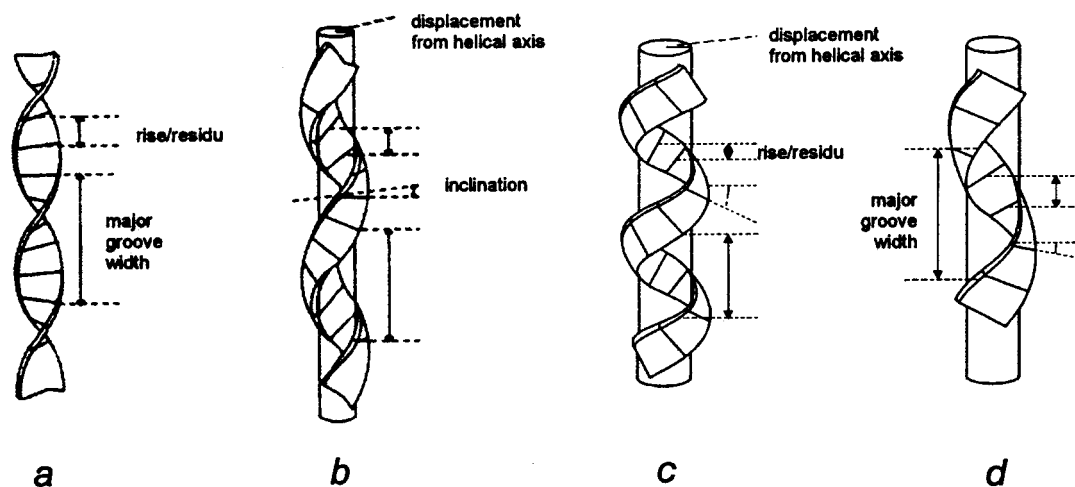
Figure 3. Ribbon analogy diagram representing B-DNA (a) and A-DNA (b) conformations together with a representation of the HNA conformations HNA-hex (c) and HNA-trig (d). The figure illustrates schematically the relationship between x-displacement (represented by a cylinder), inclination (base pairs are represented by a single line), rise, and major groove width.

Table 2. Comparison of Helical Parameters for All Cited Structures[a]

	B-DNA	A-DNA	HNA-hex	HNA-trig
x-displacement (Å)	−0.8	−4.1	−6.2	−6.5
inclination (°)	2.4	12.0	24.3	3.4
rise (Å)	3.4	2.9	2.2	3.3
twist (°)	36.1	31.1	33.2	24.2
slide (Å)	0.4	−1.6	−2.5 (−2.8[b])	−3.3 (−2.9[b])
roll (°)	0.6	6.3	11.5 (7.8[b])	4.1 (3.2[b])
major groove width (Å)	11.7	2.7	4.1	12.9
minor groove width (Å)	5.7	11.0	10.5	10.1
P···P (Å)	7.0	5.9	5.5	5.7

[a] Parameters were calculated using Curves,[31] where fitting of ideal bases was performed before the helical analysis and parameters were calculated with respect to a linear global helical axis. Groove widths were calculated by taking the shortest P···P distances and subtracting 5.8 Å to account for van der Waals radii of the phosphate groups. Average intrastrand distances between adjacent phosphates are also indicated. Data for B- and A-DNA from ref 32. [b] Average calculated excluding central step.

stacking geometries of the corresponding steps generally seem to not be influenced.

The anhydrohexitol rings adopt a chair conformation with the base in the axial position and anti conformation. The presence of the hexitol ring ensures that the torsion angle δ adopts values in a narrow range corresponding fairly well to the preferred range in A-DNA-type helices. Moreover, a narrow distribution of sugar conformations is also typically observed in A-DNA crystal structures.[29] Closely related to the sugar puckering and backbone torsional angles is the distance between adjacent phosphates of the same chain. The different sugar puckerings as observed for the different helical types imply different interphosphate distances. The C2′-endo puckering mode observed for B-type helices pushes adjacent phosphates of one chain about 7 Å apart.[30] The C3′-endo puckering of A-type helices is associated with a shorter interphosphate distance of only 5.9 Å, giving rise to underwound helices as compared to those of the B-family. Looking at both HNA structures, an even shorter interphosphate distance is found (Table 2). This is mainly due to the chair conformation of the hexitol ring striving for staggered adjacent substituents, resulting

in δ values of 69−77°, being generally lower as for typical A-type structures. The higher average δ torsion angle observed in HNA-trig as compared to that of HNA-hex results in a slightly higher mean separation between adjacent phosphates belonging to the same strand. Despite the insertion of the extra methylene group, the six-membered hexitol ring can be considered as a good mimic of a furanose ring, frozen in its C3′-endo conformation (Figure 1b).

Inspection of the helical parameters reveals for both structures a similar high x-displacement of the base pairs. These generally show nearly no propeller twisting (except the terminal base pair in HNA-trig). The base pairs are highly inclined with respect to the helical axis for HNA-hex but show almost no inclination in HNA-trig (Table 2). Moreover, the HNA-trig duplex is seriously underwound and has a higher rise when compared to HNA-hex. For HNA-trig, approximately 15 base pairs are needed to describe a full helical turn, as compared to approximately 11 base pairs for HNA-hex. The variation of these global helical parameters is correlated,[33,34] and a ribbon analogy diagram can exemplify these correlations (Figure 3). The straight twisted ribbon shown in Figure 3a represents B-DNA (no inclination and no displacement from the helical axis). When the ribbon is wrapped around a cylinder (to account for the x-displacement, Figure 3b), it could represent A-DNA where the base pairs are inclined and displaced from the helical axis. If the diameter of the cylinder is increased but the number of base pairs per turn (related to the twist) is maintained, as in the HNA-hex structure, then the ribbon will have to be wrapped more tightly (Figure 3c). The inclination increases and the rise decreases, resulting in a narrowing of the major groove width (Table 2). For the HNA-trig structure, the reduction of helical twist results in a decrease of the inclination of the base pairs and an increase of the helical rise and even the major groove width (Figure 3d). Indeed, a much higher major groove width is found for the underwound HNA-trig helix (Table 2). Despite the extremely different helical conformations, the minor groove width remains similar for both structures.

(29) Wahl, M. C.; Sundaralingam, M. *Biopolymers* **1997**, *44*, 45−63.
(30) Saenger, W. In *Principles of Nucleic Acid Structure*; Cantor, C. R., Ed.; Springer-Verlag: New York, 1984; pp 220−241.
(31) Lavery, R.; Sklenar, H. *J. Biomol. Struct. Dyn.* **1989**, *6*, 655−667.
(32) Dickerson, R. E. *Methods Enzymol.* **1992**, *211*, 67−111.
(33) Heinemann, U.; Lauble, H.; Frank, R.; Blocker, H. *Nucleic Acids Res.* **1987**, *22*, 9531−9550.
(34) Jain, S.; Zon, G.; Sundaralingam, M. *Biochemistry* **1991**, *30*, 3567−3576.

Comparison of the local helical parameters reveals the base pairs of the HNA-trig structure having on average higher slide and roll (Table 2). The difference between the average slide values for both structures however is mainly due to the different conformation of the central step of both structures. As a consequence of the specific backbone conformation localized at the central step of HNA-trig, a much higher cross-strand stacking of the adenine bases is allowed as compared with the central step of the HNA-hex structure, resulting in a significantly higher slide value. Except for this central step, very similar base stacking patterns are found for both structures. The occurrence of an intra- or interstrand stacking pattern was found to be sequence dependent where RY steps exhibit intrastrand stacking of the purine and pyrimidine rings, while YR steps prefer interstrand stacking between the purine rings. In both structures an average stacking distance between base pair planes of 3.4 Å is found, identical to what is observed in natural oligonucleotide duplexes.

The natural analogue d(GTGTACAC) also crystallizes in two crystal forms (tetragonal[35] and hexagonal[36]). In both forms the octamer was found to adopt an A-DNA structure. With the hexitol ring being a good mimic of the C3′-*endo* conformation, it is not surprising that both HNA structures share most A-DNA characteristics (see also Figure 2c). The only exception is the low value for the base pair inclination in the HNA-trig structure. In this regard, HNA-trig resembles B-DNA with the base pairs roughly perpendicular to the helical axis. A real intermediate structure possessing both A- and B-like characteristics was observed for d(CATGGGCCCATG).[37] Recently the B−A transition pathway was mapped on the basis of a set of hexamer crystal structures.[38] For both the A- and B-type structures a correlation between x-displacement and inclination is observed, with the transformation going through an extended and under-wound intermediate adopting a C3′-*endo* sugar conformation and no base pair inclination. Although this intermediate displays characteristics similar to those of the HNA-trig structure, the latter can of course not be considered as an A−B intermediate structure due to the restricted hexitol ring conformation.

The extra methylene groups of each anhydrohexitol residue facing the minor groove of HNA duplexes are also responsible for the increased hydrophobicity of this groove as compared with the minor groove of A-DNA duplexes (Figure 2d). As a consequence, the minor groove of both HNA structures is generally less hydrated. The pattern of bridging water molecules being simultaneously hydrogen bonded to adjacent phosphate groups as found for the high-resolution HNA-trig structure appears to be often encountered for A-DNA duplexes.[39] A similar hydration pattern forming intrastrand phosphate bridges has been described for the central region of the B-DNA decamer d(GGCCAATTGG) solved at 1.15 Å resolution.[40]

Symmetry-related duplexes pack by end-to-end stacking of the terminal base pairs, giving rise to continuous helices throughout the crystal. In the HNA-hex structure those continuous helices pack in parallel layers, with the helical axes rotated by 120° from one layer to the next; whereas in HNA-trig, all helical axes run in the same direction (Figure 2e). This explains also the origin of the observed crystal morphologies, being hexagonal-shaped for HNA-hex and needle-shaped for HNA-trig. Moreover, the low-twisted continuous helices in the latter case have a very wide and deep major groove, which permits the arrangement of a second continuous helix into this groove. Together, these two helices form a double helix of double helices interacting by direct hydrogen bonds between terminal hydroxyl groups and the phosphate backbone.

Conclusions

The HNA duplex structures presented here share most characteristics with the A-type nucleic acids and differ most from each other in twist, inclination, and major groove width. The number of nucleotides per full turn is for one of them close to the value of A-RNA (∼11 base pairs per turn, Figure 2c), while the other duplex is unwound to ∼15 base pairs per turn. The values of minor groove width, x-displacement, and twist observed for HNA-hex are very similar to those described for the G.C stem regions in the solution structure of h(GCGCTT-TTGCGC) as determined by NMR spectroscopy.[41] In this structure, the central four successive T.T wobble pairs cause a bending of the local helix axis and a dislocation of the helix axis of both stem regions of the duplex, which makes further comparison with the only structural information on duplex HNA difficult.

The antisense strategy requires hybridization of the antisense compound with the target mRNA. A molecular dynamics simulation study[20] and solution structure determination[15] of a HNA−RNA hybrid suggest an A-type structure with slightly different γ and ζ angles as compared to our HNA duplexes. The extensive minor groove hydration observed in the molecular dynamics study can rationalize the increased stability of HNA−RNA complexes as compared to that of HNA−DNA duplexes, but it certainly cannot explain the higher stability of HNA duplexes. As an HNA strand is designed to be conformationally more restricted than is an RNA or DNA strand,[9] the lower entropy penalty during hybridization might dominate other more minor effects, resulting in the observed higher stability of HNA duplexes. Nevertheless, a HNA strand stays flexible enough to allow crystallization in two duplex conformations. The same flexibility, of which most should be ascribed to the phosphate groups, guarantees the formation of an A-like HNA−RNA duplex after hybridization.

After two decades of crystallographic research on oligonucleo-tides, more than 500 crystal structures have been solved. Despite this large amount of structural information, the relation between sequence and a three-dimensional nucleic acid structure remains not fully understood. While in the beginning researchers tried to solve the structures of natural oligonucleotides, after a few years the impact of small modifications such as the incorporation of a modified base, sugar moiety, or phosphate group on the global structure was explored. Recently, the structures of some extensively modified oligonucleotides such as the peptide nucleic acids (PNA),[42] N3′ → P5′ phosphoramidate DNA (3′-

(35) Jain, S.; Zon, G.; Sundaralingam, M. *Biochemistry* **1989**, *28*, 2360−2364.
(36) Thota, N.; Li, X.; Bingman, C.; Sundaralingam, M. *Acta Crystallogr.* **1993**, *D49*, 282−291.
(37) Ng, H.-L.; Kopka, M. L.; Dickerson, R. E. *Proc. Natl. Acad. Sci. U.S.A.* **2000**, *97*, 2035−2039.
(38) Vargason, J. M.; Henderson, K.; Shing Ho, P. *Proc. Natl. Acad. Sci. U.S.A.* **2001**, *98*, 7265−7270.
(39) Wahl, M. C.; Sundaralingam, M. In *Nucleic Acid Structure*; Neidle, S., Ed.; Oxford University Press: Oxford, 1999; pp 133−135.
(40) Vlieghe, D.; Turkenburg, J.; Van Meervelt, L. *Acta Crystallogr.* **1999**, *D55*, 1495−1502.

(41) Lescrinier, E.; Esnouf, R. M.; Schraml, J.; Busson, R.; Herdewijn, P. *Helv. Chim. Acta* **2000**, *83*, 1291−1310.

NP DNA),[43] 2′-O-(2-methoxyethyl)-RNA (MOE-RNA),[44] and a DNA duplex with incorporated LNA units[45] have been solved, to which we now add the first crystal structure of a hexitol nucleic acid fragment. The exploration of the structure of these extensively modified structures can be of great help to gain further insight into the principles of nucleic acid structure. With this respect, it is interesting to compare HNA with the so-called homo-DNA for which the insertion of an extra methylene group occurs between the C1′ and C2′ atoms of the β-D-2′-deoxyribose unit instead of between C1′ and O4′. On the basis of NMR data, a dynamic equilibrium between two quasi-linear antiparallel double-stranded models with Watson−Crick base pairing is proposed for homo-DNA.[46] In one of the models all backbone torsion angles α to γ have a +*ap*, +*ap*, +*ap* conformation, similar to the central step in HNA-trig. The β-D-glucopyranosyl rings adopt a chair conformation with all substituents in the equatorial position. The position of the insertion has a dramatic influence on the nucleic acid structure. In the case of homo-DNA, where the base is oriented equatorial, good base stacking interactions are not possible. Short contacts between the extra methylene groups and the bases are observed, and a quasi-linear structure is adopted. For HNA however, with the bases axial, the conventional base stacking is still possible resulting in a helical conformation. This illustrates the important role of the base stacking interactions during the initial helix formation for nucleic acids. Our structural data on HNA duplexes can also be used to verify the influence of introducing substituents on the hexitol ring. An additional hydroxyl group in the α-position on the C2′ atom, giving D-altritol nucleic acids (ANA),[47] will point toward the solvent region and has no influence on the overall duplex geometry. This extra group will, however, form water-mediated bridges with close-by O1P and O3′ atoms, thereby decreasing the hydrophobicity of the minor groove wall

and increasing the sugar−phosphate backbone hydration. As a result, double-stranded ANA is even more stable than double-stranded HNA. In the case of a β-position of the hydroxyl group, a hydrogen bond with the O4′ atom of the following nucleotide was proposed for D-mannitol nucleic acids (MNA).[11] In HNA-hex we observe C2′···O4′ (next residue) distances between 2.8 and 3.4 Å, of which the shortest can be interpreted as possible C2′−H···O4′ hydrogen bonds, a type if interaction often observed in nucleic acids.[48] The intrastrand hydrogen bonding restricts the conformational flexibility too much, explaining the lower hybridization potential of MNA. The HNA structural data can also be used to model new potentially natural nucleic acids that may have occurred in a prebiotic life and may have played a role in chirality selection.

We have shown that at least one of the described HNA structures has a double helical conformation similar to double-stranded RNA, while HNA also keeps a certain degree of flexibility in solution as it is able to crystallize in two distinct forms. These properties indicate potential nanotechnological en therapeutical applications for HNA. Indeed, the local incorporation of short double-stranded HNA tracts into larger RNA structures will stabilize these regions, making, for example, the study of conformational changes in RNA or the structure determination of metastable RNA possible. Moreover, HNA can be used as potential aptamers for proteins recognizing duplex RNA.

(42) Rasmussen, H.; Kastrup, J. S.; Nielsen, J. N.; Nielsen, J. M.; Nielsen, P. E. *Nat. Struct. Biol.* **1997**, *4*, 98−101.
(43) Tereshko, V.; Gryaznov, S.; Egli, M. *J. Am. Chem. Soc.* **1998**, *120*, 269−283.
(44) Teplova, M.; Minasov, G.; Tereshko, V.; Inamati, G. B.; Cook, P. D.; Manoharan, M.; Egli, M. *Nat. Struct. Biol.* **1999**, *6*, 535−539.
(45) Egli, M.; Minasov, G.; Teplova, M.; Kumar, R.; Wengel, J. *Chem. Commun.* **2001**, 651−652.
(46) Otting, G.; Billeter, M.; Wüthrich, K.; Roth, H.-J.; Leumann, C.; Eschenmoser, A. *Helv. Chim. Acta* **1993**, *76*, 2701−2756.
(47) Allart, B.; Khan, K.; Rosemeyer, H.; Schepers, G.; Hendrix, C.; Rothenbacher, K.; Seela, F.; Van Aerschot, A.; Herdewijn, P. *Chem.-Eur. J.* **1999**, *5*, 2424−2431.

(48) Leonard, G. A.; McAuley-Hecht, K.; Brown, T.; Hunter, W. N. *Acta Crystallogr.* **1995**, *D51*, 136−139.